2007

Fracture Toughness of Ceramic Moulds for Investment Casting with Ice Patterns

Qingbin Liu

Ming-Chuan Leu
Missouri University of Science and Technology, mleu@mst.edu

Von Richards
Missouri University of Science and Technology, vonlr@mst.edu

Recommended Citation

Q. Liu et al., "Fracture Toughness of Ceramic Moulds for Investment Casting with Ice Patterns," *International Journal of Cast Metals Research*, vol. 20, no. 1, pp. 14-24, Maney Publishing, Jan 2007.
The definitive version is available at https://doi.org/10.1179/136404607X202708

Fracture toughness of ceramic moulds for investment casting with ice patterns

Q. B. Liu*, M. C. Leu and V. L. Richards

Ice patterns can be used to make ceramic investment moulds for metal castings. Owing to the characteristics of ice, the ceramic mould must be made at subzero temperatures and consequently, requires a different formulation than shells built at room temperature. Success of this process depends greatly on the fracture toughness of mould materials. The present paper describes the experimental results of fracture toughness of mould materials processed from different compositions. The Taguchi method was used to reduce the trial runs. The parameters considered included the ratio of fibre containing fused silica and aluminosilicate powders, the volume of binder and the volume of catalyst. The microstructure and green fracture surface of test bars were also examined to understand the underlying mechanism. While conducting the four point bend test on ceramic mould samples, some samples had exceedingly low strengths appearing as outliers in the Weibull analysis. Examination of these low strength ceramic samples improved understanding of failure of mould materials. Sound moulds have been made for the investment casting process with ice patterns based on the analysis of experimental results. The casting of an M8 bolt is used to demonstrate that metal castings of complex geometry can be fabricated using ice patterns. The measured tolerances are within the required tolerance range.

Keywords: Investment casting, Ice patterns, Rapid freeze prototyping (RFP), Fracture toughness

Introduction

Wax is the most commonly used material to make patterns in investment casting.[1] Stresses applied by wax as it is heated during wax removal appear to be the major cause of shell cracking. As shown by Richards and Sunderland,[2] wax behaves as a partially crystalline linear polymer and exhibits an abrupt increase in volume during dewaxing. This expansion is the source of stress that tends to cause shell cracking during the autoclave step of investment casting mould preparation. In contrast, ice exhibits contraction upon melting. Use of ice patterns may alleviate investment shell cracking as illustrated in Fig. 1.

The freeze cast process (FCP) is an investment casting process patented by Yodice.[3] In this process, ice patterns are used instead of wax patterns to make metal parts. Yodice and others have demonstrated the feasibility of investment casting with ice patterns.[4–6] The advantages of FCP over the competing casting processes include low cost, high quality and fine surface finish. These strengths make FCP a significant alternative to the traditional investment casting for production of quality near net shape castings at reasonable cost. Complex, three-dimensional patterns can be fabricated by using the rapid freeze prototyping (RFP) process, in which patterns are directly built from a CAD model by freezing water droplets layer by layer.[7–10] Because of the use of ice, the moulding process must be performed below water freezing temperatures. Therefore, mould materials must exhibit specific characteristics and the design requires extensive knowledge of the properties of mould materials. Although investment casting with ice patterns has been developed for quite some time, very few publications have discussed the properties of ceramic moulds that are suitably formulated to be made in a low temperature environment.

Previous experimental results show that the moulds made are prone to cracks during curing, as shown in Fig. 2*a*. Success of this process therefore depends greatly on the adequate fracture toughness of chosen mould materials. Therefore, a fracture toughness study using fractography has been conducted. In the present paper, the selection of the ceramic powder, binder and catalyst material for ceramic slurry preparation in the mould making process is first introduced. The experimental results of the fracture toughness of mould materials with different compositions are then described. The Taguchi method is used to reduce the number of trial runs. The parameters considered include the ratio of fibre containing fused silica and aluminosilicate refractories, the volume of binder and the volume of catalyst. Analysis of variance for fracture toughness is performed to evaluate the significance of the effect of each parameter. The microstructure of mould materials and the green

Department of Mechanical and Aerospace Engineering, University of Missouri–Rolla, 1870 Miner Circle, Rolla, MO 65409-0050, USA

*Corresponding author, email qbliu@yahoo.com

Received 15 November 2005; accepted 12 April 2007
DOI 10.1179/136404607X202708

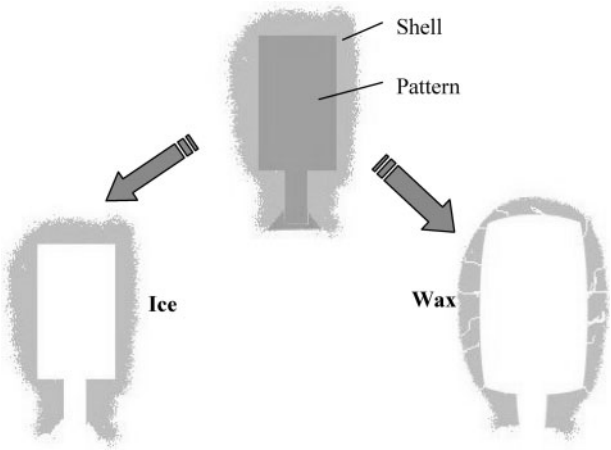

1 Use of ice patterns may alleviate investment shell cracking

fracture surface of test bars are also examined to determine the underlying fracture mechanism. The casting of an M8 bolt is used to demonstrate that metal castings of complex geometry can be fabricated using ice patterns.

Choice of material for low temperature investment moulding

Some materials used for investment casting with ice patterns will have different characteristics from those used for regular investment casting with wax patterns.[11–15] For example, the binder solution for investment casting with ice patterns should contain no water and should not freeze at subzero temperatures. Materials for binder, ceramic powder and catalyst used to make moulds for investment casting with ice patterns are discussed in this section.

Ceramic materials

The slurry is made of a mixture of binder and ceramic materials. Therefore, these materials play an important role in successful mould or shell making. In general, refractories are used in a very wide range of combinations and include silica sand, aluminosilicates, alumina, fused silica and zirconium silicate. Choosing appropriate ceramic materials is essential to produce smooth surface finish, high dimensional accuracy and good properties of the metal castings. The following factors need to be considered when choosing the ceramic materials: refractoriness, thermal expansion coefficient, chemical composition, cost, particle size distribution and application. A ceramic material usually has several particle sizes with a certain mixing ratio for shell making. The ratio of fine/medium/coarse powder is critical to shell quality. Because of the authors' interest in fabricating small parts, the aluminosilicate was selected first. However, the moulds exhibited low strengths and easily cracked as shown in Fig. 2*a*. Thus, the fibre containing fused silica was employed to generate crack free moulds as shown in Fig. 2*b*. The detailed experimental results will be discussed below.

Binder

Another major slurry component is the binder, which is mixed with ceramic particulate material to make the slurry. For low temperature investment casting, the binder solution should not freeze and should have good fluidity at subzero temperatures, and the corresponding mould or shell must have good surface finish, high accuracy and high strength. These are the criteria used in choosing binder materials in the present application. In general, three kinds of binder materials can be chosen: water glass, silica gel and ethyl silicate. The mould or shell made with the water glass binder has low high temperature strength. Moreover, the dimensional accuracy of the corresponding metal castings is relatively low and the surface finish is relatively poor. Thus, water glass is not used in the present study. Silica gel is made from water glass by dilution with 9–10 times water followed by partial evaporation. The silica gel contains 40–50 wt-% water and it will freeze in a subzero environment. Therefore, silica gel is also not used in the present study.

Ethyl silicate satisfies all of the above requirements for the binder. Pure ethyl silicate can be used to produce a foundry binder but it is more common to employ a condensed or concentrated form containing a certain percentage of silica, for example, 40 wt-%. Pure tetraethyl orthosilicate has no binding properties, but it must be chemically decomposed by reacting with water, i.e. hydrolysed.[1] This should produce a network of amorphous silica that will serve as the binder. Because ethyl silicate is not soluble in water, the reaction only occurs at the interface and thus is slow. Alcohol is soluble in both ethyl silicate and water. By adding alcohol, the reaction speed can be substantially increased. The binder is alcohol based and free of water after chemical reaction because all the available water has been used up in the

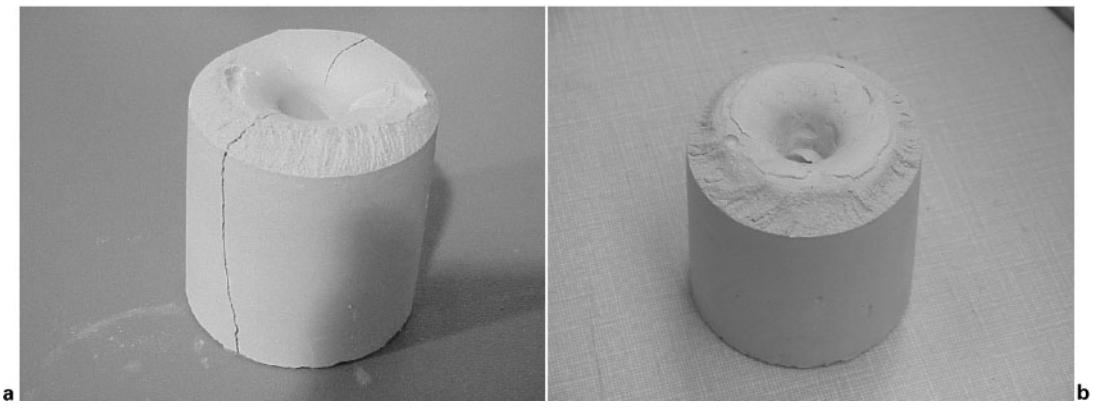

2 Solid investment moulds made *a* without and *b* with fibre containing fused silica

hydrolysis. The chemical process of hydrolysis can be accelerated by the addition of a small amount of acid, which acts as a catalyst.

Catalyst

To shorten the gelling time of the slurry (mixture of binder and ceramic material) for low temperature investment casting, a catalyst is used. Otherwise, it will take days or longer for the slurry to gel. In general, the time mainly depends on temperature, binder composition and the pH value. The effect of pH is more significant than the other two factors. The slurry is most stable when the pH value is equal to 2, thus the gelling time is the longest when pH=2. On the other hand, the slurry is most unstable and the corresponding gelling time is much shorter when the pH value is between 5.0 and 6.0. When the pH value is <1.0, the slurry is also unstable. The aim of adding a catalyst is to change the pH from the stable range to the unstable range. Based on the above arguments, it can be seen that the catalyst can be either acid (to change the pH value towards 1.0) or alkaline (to change the pH value towards 6.0).

The most commonly used acid catalysts include H_2SO_4, HCl and H_3PO_4, while NaOH, $Ca(OH)_2$, MgO, CaO, $Mg(OH)_2$, Na_2CO_3 and various organic amines are among the alkaline catalysts that can be used. From the experimental results shown in Ref. 6, it can be seen that the use of an organic catalyst can result in a high quality ceramic shell or mould with high mechanical strength and good surface finish. An inorganic catalyst remains inside the ceramic shell or mould after firing, deteriorating the high temperature mechanical performance. Also, the inorganic residue will promote devitrification of the bond phase causing cracking and CO_2 bubbles, which affect the surface quality. An organic catalyst is active and will be evaporated or burnt out during the firing process; thus, it has no effect on the high temperature performance of the ceramic shell or mould. The results in Ref. 6 show that triethanolamine has good performance when used as a catalyst, so a mixture of triethanolamine and alcohol is employed in the present study.

Slurry system

The slurry system contains ceramic powder, binder and catalyst. The ratio of these three components is important to the performance of the slurry system, the building of ceramic shells or moulds and consequently, the quality of castings. Therefore, a correct mixing ratio among the three components is critical to controlling the accuracy and surface finish of castings.[1]

Table 1 Particle size distribution of fused silica

Particle size, μm	Percentage, wt-%
850	0.025
600	1.520
425	2.090
300	1.738
250	0.000
180	0.299
150	8.640
106	6.633
75	8.447
45	13.763
Pan	56.845

Table 2 Particle size distribution of aluminosilicates

Particle size, μm	Percentage, wt-%
200	2.15
150	5.28
100	11.91
75	15.09
50	12.99
25	21.07
Pan	31.51

Based on the discussion above, the following materials were chosen: a mixture of aluminosilicate (M47-200ICC, Ransom and Randolph Co.) and fibre containing fused silica (Nalcast, Nalco Chemical Co.) as the ceramic powder, alcohol based prehydrolysed ethyl silicate (binder #18, Ransom and Randolph) as the binder and a mixture of triethanolamine and ethanol (1 : 1.5 volume ratio) as the catalyst. The particle size distributions of fused silica and aluminosilicates are shown in Tables 1 and 2 respectively. To ensure repeatable results, the following precautions were taken:

(i) the binder batch was isolated in a carboy with a bung pump and a Drierite column on the vent so the headspace is kept with low moisture content. Before use, the binder was put inside the freezer to precool to the environment temperature in a sealed bottle
(ii) ceramic powders are dried for 2 h at 240°C to control the moisture content regardless of storage history and kept in a sealed jar in the freezer before use
(iii) triethanolamine and ethanol are mixed first according to the volume ratio stated above and stored in a sealed bottle inside the freezer before use
(iv) the amount of each material, i.e. catalyst, binder and ceramic powder, was precisely measured.

Experimental procedure

Processing parameters

Three parameters were chosen in the present study: the amount of catalyst, the amount of binder and the ratio of fibre containing fused silica to aluminosilicate. Three levels for each of these parameters were selected, as shown in Table 3. To reduce the number of trial runs, the Taguchi method of experiment design was used as an L9 orthogonal array. The set of experimental parameters and the corresponding solid loadings (vol.-%) are listed in Table 4. The weights of fused silica and aluminosilicate powders used are shown in Table 4. The three levels of each parameter were chosen to be within reasonable ranges based on the authors' previous experience. The mixing time is kept constant (4 min) in

Table 3 Processing parameters and corresponding levels

	Level		
Parameter	1	2	3
Aluminosilicate/fused silica, g	325/25	325/50	325/75
Binder, mL	130	140	150
Catalyst, mL	8	10	12

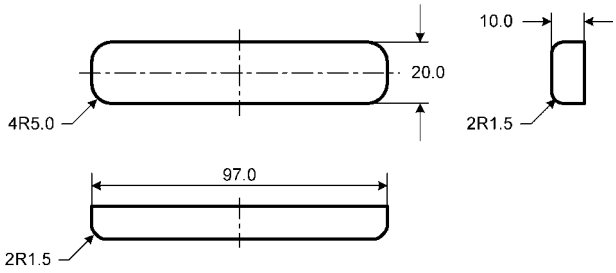

3 Dimension of moulded test bar, mm

the present study. The choice of mixing time was based on a large number of experiments conducted previously.

Sample preparation

Test bars were made by slip casting of the ceramic slurry into ice moulds, followed by melting of the ice to allow sample removal. The following procedure was used to mix the ingredients:

(i) predried powders, once removed from the freezer, are weighed and placed in the mixing bowl of the vacuum mixer
(ii) the binder is measured using a precooled measuring cup and poured into the mixing bowl at the freezer temperature
(iii) the premixed catalyst is then added into the mixing bowl. The catalyst is measured using a precooled graduated cylinder, then poured into the mixing bowl
(iv) the precooled mixing bowl is capped and attached to the vacuum mixer, then stirring starts. The vacuum mixer used is the Pro Blend mixer (Whip Mix Corporation)
(v) immediately after the mixing, the slurry is poured into the ice mould to make the test bar. Before mixing, all the materials are kept at the environment temperature inside the freezer, i.e. -15°C. At the end of mixing, the slurry temperature can rise to -4°C.

The geometry and dimensions of the designed test bar are illustrated in Fig. 3. The design of the test bar is based on the ASTM standard C1161-02c, which has been modified to take into account the low strength of the gelled slurry.[16–18] The side of the test bar placed in tension during the test was that in contact with the ice mould during manufacture (no post-processing done to it). After the gellation, the test bars were fired as per a standard investment mould. The length and thickness of each bar were measured using a Mitutoyo electronic digimatic caliper and recorded. The samples were then fractured using the four point bend apparatus.

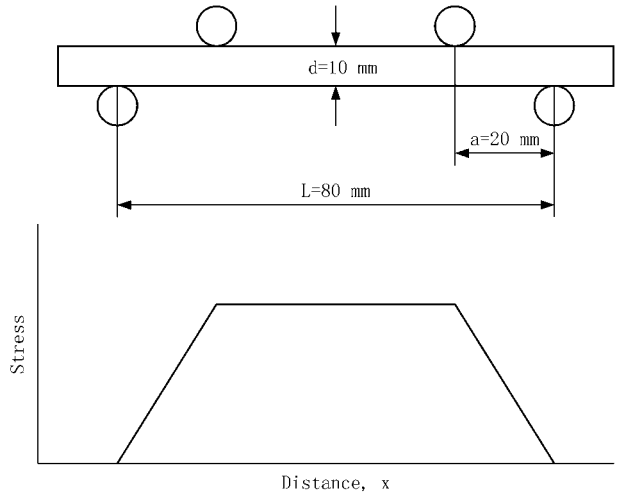

4 Stress distribution in four point bend testing

Four point bend test

A four point bend apparatus adapted to an electronic universal sand strength machine (Simpson Technologies Corporation) was used. The four point bend method subjects the tensile portion of the sample to a uniform stress over a specified region, as shown in Fig. 4. A fully equalised fixture was built following the concepts of error reduction in ceramic testing proposed by Baratta.[17] The load required to fracture the bar is recorded. Data for bars that fail at or outside the four load points were considered suspect and omitted from the statistical analysis. For each sample parameter, 15–20 bars were tested. The standard formula for the strength of a beam in four point-1/4 point flexure is as follows, where the load points are spaced 1/4 of the rest span in from the rest points

$$S = \frac{3PL}{4bd^2} \quad \text{(MPa)} \tag{1}$$

where P is the breaking force, L is the distance between outer spans, b is the specimen width and d is the specimen thickness. All these dimensions were shown in Figs. 3 and 4. The fracture surface was kept intact after the testing. The loading rate of the tester was 120 ± 10 PSI min^{-1}. Fractographic studies are then performed on the low strength bars obtained from the four point bend test. The Weibull modulus was calculated from the four point bend test results.

Fractography

The fracture surface obtained from the four point bend test piece was observed under a digital microscopic camera (Polaroid digital microscope camera 2.0), along

Table 4 Taguchi experimental matrix and corresponding solid loading

Experiment no.	Aluminosilicate/fused silica, g	Binder,mL	Catalyst, mL	Solid loading, vol.-%	Weibull modulus
1	325/25	130	8	48.99	10.99
2	325/25	140	10	46.91	7.79
3	325/25	150	12	45.00	5.75
4	325/50	130	10	50.35	9.77
5	325/50	140	12	48.29	4.41
6	325/50	150	8	47.33	5.13
7	325/75	130	12	51.60	5.78
8	325/75	140	8	50.57	7.59
9	325/75	150	10	48.62	6.06

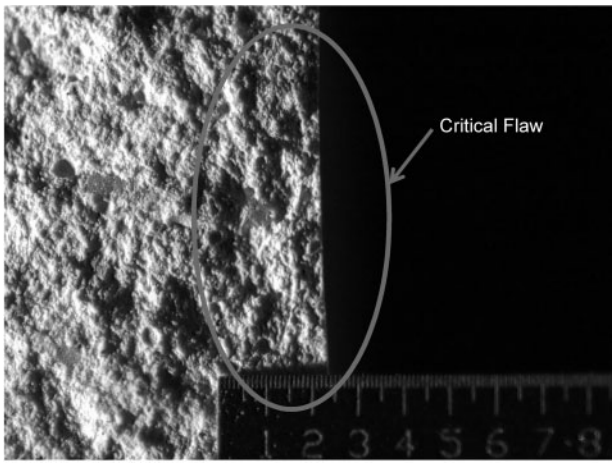

5 Fractography of broken bar showing critical flaw: unit on scale is 1 mm

with a microscopic scale. An oblique lighting source was used, where light was incident at an inclined angle to the fracture surface of the sample. The critical flaw which resulted in fracture was identified. An example is shown in Fig. 5. The flaw dimensions were measured from the smooth tensile surface of the bar to an area that was most clearly connected to the other fracture surface before fracture occurred. A Scion image analyser was used to improve the measurement accuracy. The fracture toughness was calculated using the equation shown in the later section based on crack dimensions and the measured four point tensile stress.

SEM samples

A Hitachi S-570 LaB_6 scanning electron microscope was used to examine polished samples and green fracture surfaces of test bars. The test bar was sectioned and embedded inside an epoxy material (EPO-fix embedding resin, Electron Microscopy Sciences) for polished section preparation. After polishing, the test bar was sputter coated with Au–Pd to make the material conductive. For SEM of a green fracture surface, the intact fracture surface was sputter coated with Au–Pd, then glued on the mount using carbon paint to further improve the conductivity.

Investment casting procedure

In general, the procedure of investment casting with ice patterns is similar to that of investment casting with wax patterns, but pattern making and demoulding are done in a low temperature environment. The procedure was as follows:

(i) fabricate ice patterns using either silicone moulds or a rapid freeze prototyping machine
(ii) prepare ice components for the runner and sprue. Assemble the ice patterns, runner and sprue together to make a pattern tree
(iii) coat the pattern tree with an interface agent either by immersing it into the liquid interface agent or by spraying the liquid interface agent onto its surface. Detailed information can be found in Refs. 11–14
(iv) prepare the ceramic slurry and pour the slurry around the pattern tree allowing to gel to make a mould
(v) after the gellation of the slurry, take the mould out of the freezer and put it in room temperature to melt the ice pattern, then drain the water

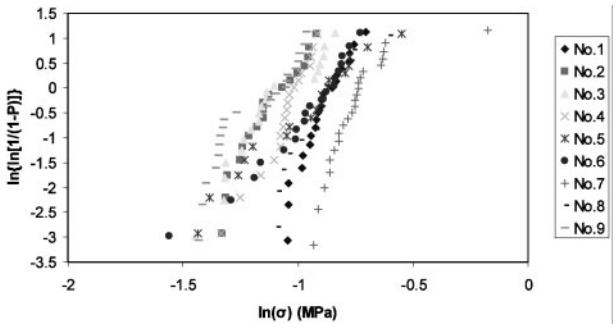

6 Determination of Weibull modulus for each trial

(vi) heat the mould to 900°C in the furnace for 4 h to fire the mould
(vii) preheat the cast alloy and move the preheated alloy from the furnace onto the holder of a centrifugal casting unit, then completely melt the alloy and cast
(viii) remove the refractory and cut off the metal castings.

A Fornax T centrifugal cast machine (Bego Company, Germany) was used in the present study to cast metal parts. An Insultherm 900 furnace (KerrLab) was used to preheat and fire the ceramic mould.

Results and discussion

Fracture toughness

Considerable scatter exists in the values of breaking strength of ceramic materials obtained from bend test results based on the Taguchi matrix. To test the degree of reliability of ceramic materials, it is necessary to use statistical tools to characterise and compare the variability. The Weibull modulus m is employed in this study, given as follows[19,20]

$$\ln\ln\frac{1}{1-P} = m\ln\sigma - m\ln\sigma_c + \text{constant} \quad (2)$$

where σ is the stress rupture and σ_c is the characteristic stress, which depends on the distribution function best fitting the data. The probability of failure P is estimated as $p/(q+1)$, where p is the rank order of samples according to strength and q is the total number of samples tested. The Weibull modulus is obtained by plotting $\ln\ln[1/(1-P)]$ as a function of $\ln\sigma$, performing a linear regression, and calculating the slope of the straight line. Better material homogeneity is shown by higher values of the Weibull modulus. Some samples seem to have exceedingly low strengths, appearing as outliers in the Weibull analysis, as shown in Fig. 6. Examination of these low strength samples can help understand the failure of ceramic moulds. Fractography analysis was used to analyse the fracture features of these samples and relate them to causes of fracture. This method is an unconventional way of determining fracture toughness. The calculation of plane strain fracture toughness is important for understanding the material characteristics. Once the fracture toughness is determined, the sensitivity of the material to process flaws can be more thoroughly understood.[21] The assumption here is that for a linearly elastic material, the bimodal distribution of strength really represents a distribution of flaw sizes. Therefore, the mode with the lowest strength was selected for analysis because the

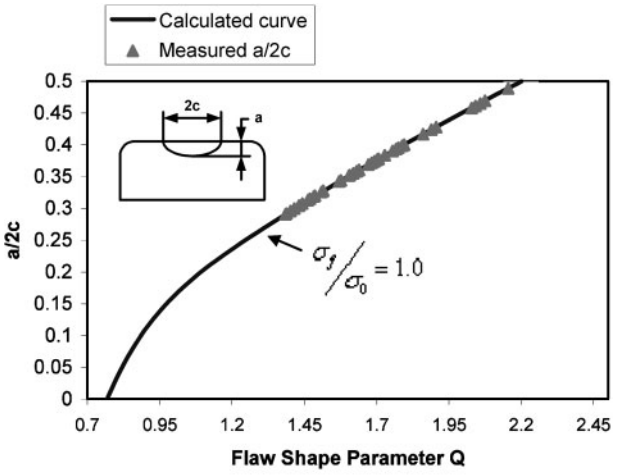

7 Flaw shape parameter *Q* for surface elliptical cracks[22]

largest flaws can be measured, thus improving the percentage precision of the flaw size measurement. Also, by looking at the most damaging flaws, it is sometimes possible to identify their sources and improve the process.

In brittle fracture, the presence of cracks or crack-like defects leads to unstable rapid failure when the stress at the crack tip exceeds a critical value. This critical value, called the plane strain critical stress intensity, is the property of a material that imparts resistance to failure in the presence of a crack-like defect. It is also referred to as fracture toughness. The relationship between fracture toughness K_{IC} and crack length is given by Ref. 22

$$K_{IC} = Y\sigma_f(\pi a)^{1/2} \quad \left(\text{MPa m}^{1/2}\right) \tag{3}$$

where Y is a geometric constant, σ_f is the tensile strength, which is the stress causing crack propagation, and a is the depth of an edge crack. The fracture stress σ_f is obtained from the four point bend test. The geometric factor Y is dependent on the specimen and crack geometry. For a semi-elliptical surface crack with the major plane of crack perpendicular to the applied tensile stress (as shown in Fig. 5), fracture toughness K_I is given by Refs. 22–24

$$K_I^2 = \frac{1{\cdot}21a\pi\sigma_f^2}{Q} \quad (\text{MPa}^2\ \text{m}) \tag{4}$$

where Q is the flaw shape parameter and $Q = \phi^2 - 0{\cdot}212(\sigma_f/\sigma_0)^2$, where ϕ is an elliptic integral of the second kind and σ_0 is the yield strength. In brittle materials, the yield strength is equal to the tensile strength, therefore $\sigma_f/\sigma_0 = 1$. Figure 7 shows the flaw shape parameter Q, plotted against the crack shape ratio $a/2c$, where $2c$ is the width of the crack.[22] After the measurement of the crack depth and width (as shown in Fig. 7), the flaw shape parameter Q can be obtained from the crack shape ratio $a/2c$. The fracture toughness can then be calculated using equation (4). Table 5 shows the calculated values for fracture toughness and breaking strength obtained from the experimental trials. Compared with the data shown in Ref. 21, the data in the present paper is within the lower end of the range of values reported for investment casting ceramics. The precracking method with a microhardness indenter was

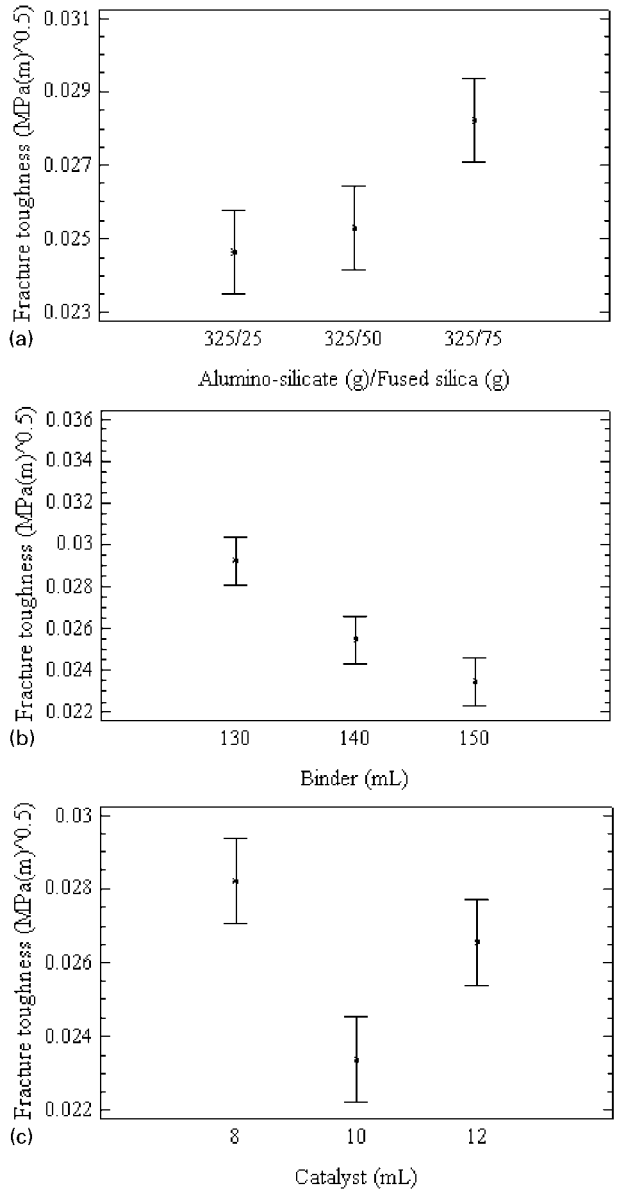

***a* mean fracture toughness and 95% confidence interval for different fused silica/aluminosilicate ratios; *b* mean fracture toughness and 95% confidence interval for different volumes of binder; *c* mean fracture toughness and 95% confidence interval for different volumes of catalyst**

8 Effect of different parameters on fracture toughness

tried and dye prenetrant was used to help identify the flaws in the authors' previous work. Owing to the permeability of the ceramics, the dye penetrant was very confusing. Additionally, a high loss of samples due to fracture during the indentation process was experienced. As shown in Ref. 21, the fractography using the native flaw population was more precise than the indentation method if based on the standard deviation as a crude measure of precision.

Figure 8 shows the measured dependence of fracture toughness on the ratio of fibrecontaining fused silica *v.* aluminosilicate, the amount of binder and the amount of catalyst. To study the significance of the effect of each parameter, the analysis of variance (ANOVA) was employed to quantitatively estimate the relative contribution of each parameter to the fracture toughness.[25] ANOVA uses sum of squares to quantitatively examine

Table 5 Calculated values for fracture toughness and breaking strength

Trial run no.	Sample no.	Fracture toughness K_{IC}, MPa $m^{1/2}$	Breaking strength, MPa
1	1-15	0.0270872	0.374
	1-18	0.0295864	0.376
	1-20	0.0281261	0.352
	1-21	0.0272221	0.353
	1-22	0.0299234	0.353
2	2-5	0.0207475	0.265
	2-6	0.0213137	0.271
	2-20	0.0256051	0.286
	2-21	0.0216225	0.269
	2-22	0.0255214	0.289
3	3-4	0.0230653	0.269
	3-6	0.018399	0.235
	3-7	0.0241757	0.288
	3-13	0.0244313	0.268
	3-16	0.0227795	0.267
4	4-2	0.02732	0.332
	4-3	0.0255554	0.286
	4-6	0.0202759	0.264
	4-17	0.0284603	0.313
	4-23	0.0275361	0.341
5	5-1	0.0236127	0.251
	5-3	0.0197353	0.238
	5-6	0.0283403	0.292
	5-14	0.0254032	0.302
	5-16	0.0209927	0.255
6	6-3	0.0276234	0.313
	6-5	0.0254126	0.275
	6-6	0.018689	0.21
	6-10	0.0321695	0.346
	6-11	0.0282985	0.305
7	7-1	0.0314959	0.402
	7-13	0.0370882	0.422
	7-14	0.0327425	0.394
	7-16	0.0330385	0.412
	7-19	0.033037	0.422
8	8-1	0.0302844	0.336
	8-2	0.0327597	0.353
	8-6	0.0271887	0.344
	8-10	0.0307347	0.371
	8-12	0.0282549	0.337
9	9-1	0.0198617	0.243
	9-3	0.0238115	0.258
	9-4	0.0200665	0.239
	9-17	0.0212505	0.261
	9-19	0.0217044	0.247

the deviation of the control factor effect response averages from the overall experimental mean response. The total variation in all of the measurements can be divided into two separate components: the variation due to the effects of the control factors and the variation due to the errors. An F ratio can be formed based on the control factor effect variance and experimental error variance. A P value can be obtained corresponding to the calculated F ratio, which is a measure of evidence against the null hypotheses. Null hypothesis is typically statement of no difference or effect. A P value close to zero signals that the null hypothesis is false and typically that a difference is very likely to exist. Large P values close to 1 imply that no detectable difference exists for the sample size used. A P value of 0.05 is a typical threshold used in industry to evaluate the null hypothesis. Table 6 shows the result of analysis of variance for the fracture toughness. Because all three P values are <0.05, these factors will have statistically significant effects on fracture toughness at the 95% confidence level. Figure 8*a* shows the effect of the ratio of fibre containing fused silica and aluminosilicate on fracture toughness. Again, the actual amounts of aluminosilicate and fibre containing fused silica are provided (rather than

Table 6 Analysis of variance for fracture toughness

Source	Sum of squares	Mean squares	*F* ratio	*P* value
Binder	2.58×10^{-4}	1.29×10^{-4}	13.43	0.0000
Catalyst	1.82×10^{-4}	9.10×10^{-5}	9.45	0.0005
Fused silica/aluminosilicate	1.09×10^{-4}	5.45×10^{-5}	5.67	0.0070
Residual	3.66×10^{-4}	9.62×10^{-6}	–	–
Total	9.15×10^{-4}	–	–	–

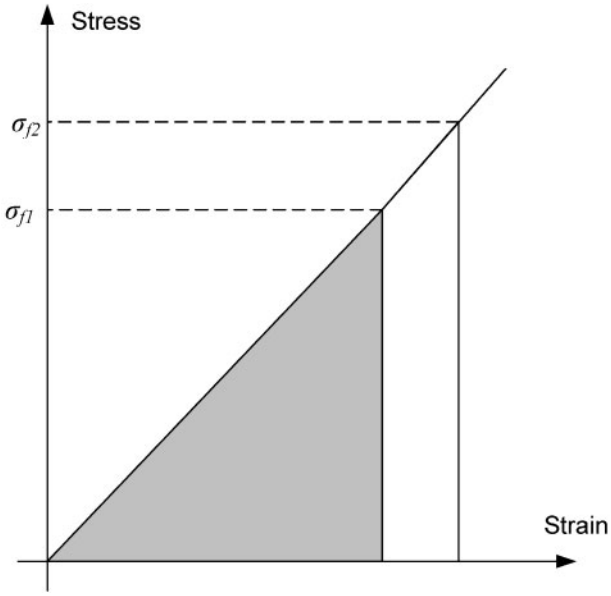

9 Schematic illustration of calculation of work of fracture

the ratio of fibre containing fused silica and aluminosilicate). The mean fracture toughness increases with an increase in the proportion of fibre containing fused silica. The analysis of variance suggests that a statistically significant difference does not exist when the amount of fused silica is 25 g versus 50 g. However, a statistically significant difference exists when the amount of fibre containing fused silica is increased to 75 g. This suggests that when the amount of fibre containing fused silica is 75 g, the fracture toughness is much higher than when the amount of fibre containing fused silica is 25 or 50 g. The result also implies that the fracture toughness can be substantially improved when the added fibre containing fused silica is larger than a critical value. When the proportion of fibre containing fused silica is less than a critical value, the effect of the fibre containing fused silica is insignificant. Figure 8*b* shows the effect of the amount of binder on the fracture toughness. A higher amount of binder results in a lower fracture toughness because of the decrease of solids loading, causing an increase in pore volume. For a brittle material, the decrease in the area of the load bearing cross-section causes an apparent decrease in fracture energy. Figure 8*c* demonstrates the effect of the amount of catalyst on the fracture toughness. It is difficult to draw a conclusion for this parameter. More experiments need to be performed to investigate the effect of the amount of catalyst on the fracture toughness.

As stated above, the key to enhancing the fracture toughness of mould materials appears to be related to the addition of fibre containing fused silica into slurry systems. The improvement of fracture toughness of specimens with the addition of polymer fibres can be explained by two mechanisms. First, the powdered materials have a wide range of particle size distribution. Fine particles can fill in the gaps between coarse particles. A higher ratio of fibre containing fused silica *v.* aluminosilicate leads to a higher solids loading. This improves the green packing, resulting in a higher density and a larger load bearing area for any cross-section. Thus, the strength increases, causing the fracture energy

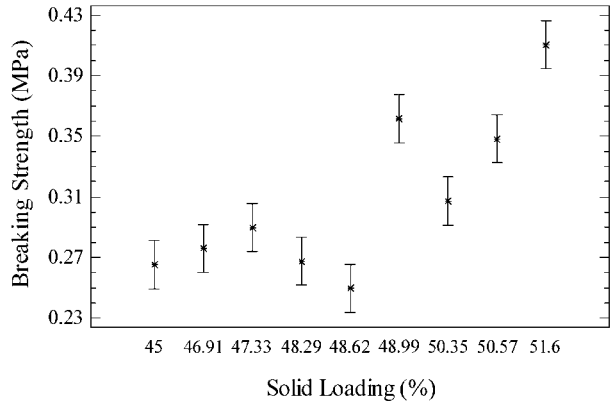

10 Effect of solids loading on breaking strength

to increase. Work of fracture can be represented by the triangular area under a stress–strain curve as shown in Fig. 9. It can be seen that work of fracture is determined by the strength and elastic modulus (slope of the hypotenuse) of the material. If the slope of the hypotenuse (modulus) is constant, a larger breaking strength will result in a higher work of fracture and consequently, a higher fracture toughness. Figure 10 shows the effect of solids loading on breaking strength. The breaking strength appears to dramatically increase when the solids loading is larger than a certain value. Figure 11 illustrates the correlation between fracture toughness and breaking strength. The linear relationship suggests a constant modulus. Therefore, a higher solids loading results in a higher work of fracture and a higher fracture toughness. Second, the improvement is due to crack deflection. Fibre additions enhance the green toughness by the pullout and modulus transfer mechanisms.[26] After the firing, the voids in the mould left by the burning out of fibres can act as crack deflectors. Crack deflection usually takes place when local areas have lower resistance to crack propagation than an average plane cutting through right angles to the tensile stress.[21,26] Crack deflection is based on the tilting and twisting of crack planes due to the residual voids left by the polymer fibres. The stresses acting in inclined planes near a crack tip depend on the angles involved. For straight cracks, the tilt is about a direction perpendicular to the crack advance through an angle θ. The stress intensity factor required for crack propagation is given by[21]

$$K(\theta) = K_o \sec^2(\theta/2) \quad \text{(MPa)} \tag{5}$$

where K_0 is the plane strain stress intensity at $\theta=0^\circ$. Crack propagation is diverted by a layer of porous

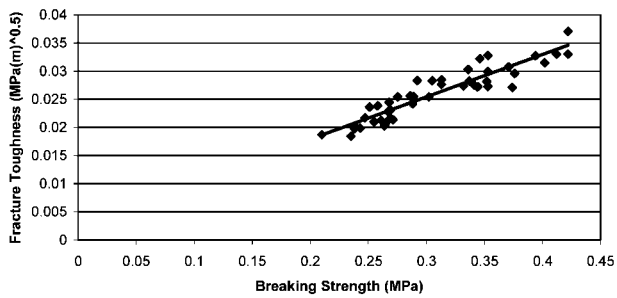

11 Correlation between fracture toughness and breaking strength for sample shown in Table 5

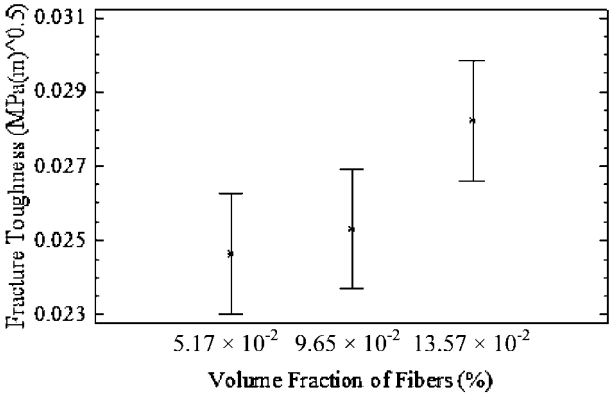

12 Effect of volume fraction of fibres in powders on fracture toughness

structure due to the addition of polymer fibres and the effective stress intensity at the diverted crack tip is lessened. This makes the apparent critical stress intensity for a crack perpendicular to the applied stress higher. Thus, the more added fibre containing fused silica, the more the residual voids left by the polymer fibres. Figure 12 demonstrates the effect of volume fraction of fibre contained in powders on fracture toughness.

SEM analysis

Figure 13 illustrates an SEM image showing the green fracture surface of a fibre modified ceramic mould. It can be seen that the fibre additions stay intact, thus enhancing the green strength of mould material because of the pullout and modulus transfer mechanism. After the firing, the voids in the mould left by the burning out of fibres can act as crack deflectors. As a crack propagates through the test materials, contact with a void results in crack tip stress intensity reduction and crack direction change, resulting in higher toughness values.

The powdered materials used in the experimentation contain particles with a large size distribution, illustrated by the microstructure of a test bar shown in Fig. 14. The dimension of the biggest particle approaches 200 μm and a small portion of particles are ~100 μm in diameter. Most of particles are fine particles (below 25 μm) filling the gaps between relatively bigger

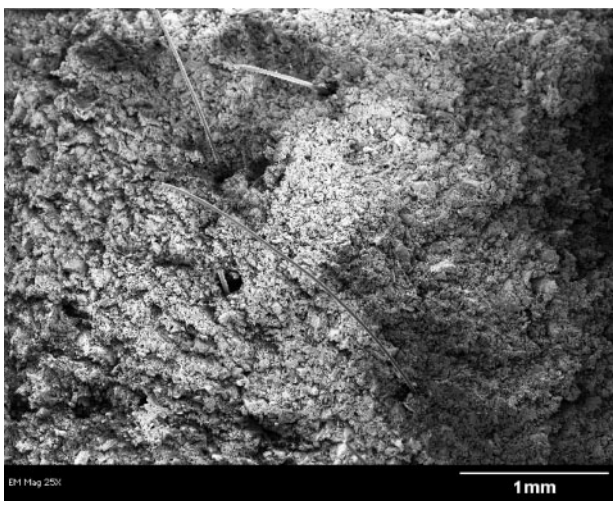

13 Scanning electron microscopy image of ceramic mould showing evidence of fibre pullout

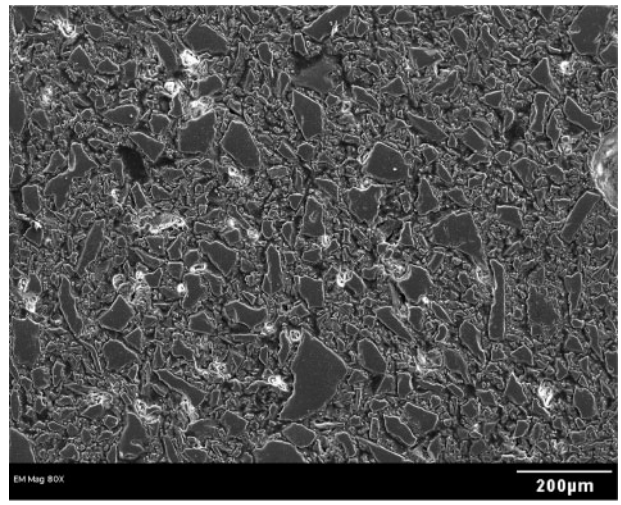

14 Microstructure of fired test bar

particles. Those very fine particles shown in the figure originate either from powdered materials or have precipitated from the binder. Overall, the material microstructure is dense with reduced porosity, thus improving resistance against fracture.

Dimensional tolerances

Based on the experimental results and analyses above, the following composition was selected to make ceramic slurries for crack free moulds: 325 g aluminosilicate, 50 g fused silica, 130 mL binder and 8 mL catalyst. This composition works well in the investment casting with ice patterns. An M8 bolt was used to demonstrate that metal castings of complex geometry and fine features can be fabricated using investment casting with ice patterns. Figure 15 shows the threads of an M8 bolt obtained from the investment casting process. The outer diameter (OD), depth of thread h and thread pitch p of the metal castings were measured and compared with those of the metal bolt used to make a mould for the ice patterns. The nominal outer diameter of the bolt OD_{nom} was 7.78 mm. The nominal depth of thread h_{nom} and the nominal thread pitch p_{nom} were 0.812 and 1.25 mm respectively. The outer diameter of bolt castings was measured using a digital caliper. The depth of thread and the thread pitch were obtained by taking pictures of threads under a scanning electron microscope and measuring them using a Scion image analyser.

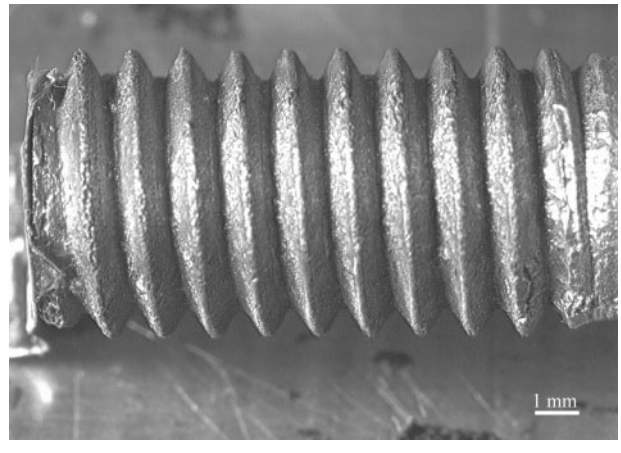

15 Threads of metal casting for M8 bolt

Tables 6–8 show the measured results and corresponding shrinkage.

Beeley and Smart[1] have derived an equation for calculating a tolerance for investment casting using wax patterns as follows

$$T = \pm(0{\cdot}13 + 5D/1000) \quad \text{(mm)} \tag{6}$$

where T is the casting tolerance and D is the dimension being compared. It should be noted that Beeley and Smart's equation does not take into consideration the alloy used and is for wax patterns. For the M8 bolt, the tolerances for the outer diameter, thread pitch and depth of thread were ± 0.17, ± 0.14 and ± 0.13 mm respectively. The US Investment Casting Institute has suggested the use of ± 0.17 mm tolerance for dimensions up to 10 mm for investment casting processes using wax patterns.[27] To determine whether the dimensions obtained in the present experimentation are within the desired tolerance range, the following equation is employed

$$Cp = \frac{|\text{USL} - \text{LSL}|}{6\sigma} \tag{7}$$

where σ is the standard deviation, USL and LSL are the upper and lower specification limits based on Beeley and Smart's equation respectively. In this case, the Cp values for the three parameters are all >1, indicating that the process capability is better than the tolerance calculated from Beeley and Smart's equation according to the six sigma concept. All the data points fall within the desired limits of distribution, thus making the process repeatable.

The ice pattern of the bolt was made using a silicon rubber mould. No shrinkage compensation was provided for the pattern. This has led to an obvious systematic error in the generated castings. It can be seen from Tables 7–9 that the mean shrinkages for the outer diameter, thread pitch and depth of thread are 2.069,

Table 7 Measured outer diameter and corresponding change (OD_{nom}=7.78 mm)

No.	OD, mm	$\Delta OD = OD_{nom} - OD$, mm	Reduction in OD, %
1	7.68	0.1	1.29
2	7.64	0.14	1.80
3	7.61	0.17	2.19
4	7.6	0.18	2.31
5	7.61	0.17	2.19
6	7.6	0.18	2.31
7	7.64	0.14	1.80
8	7.56	0.22	2.83
9	7.63	0.15	1.93
10	7.62	0.16	2.06
Average	7.619	0.161	2.069
Standard deviation	0.032	0.032	0.408

Table 8 Measured thread pitch p and corresponding change (p_{nom}=1.25 mm)

No.	Thread pitch p, mm	$\Delta p = p_{nom} - p$, mm	Change, %
1	1.302	−0.052	−4.16
2	1.297	−0.047	−3.76
3	1.291	−0.041	−3.28
4	1.302	−0.052	−4.16
5	1.298	−0.048	−3.84
6	1.295	−0.045	−3.6
7	1.316	−0.066	−5.28
8	1.314	−0.064	−5.12
9	1.293	−0.043	−3.44
10	1.329	−0.079	−6.32
Average	1.3037	−0.0537	−4.296
Standard deviation	0.0122	0.0122	0.9733

Table 9 Measured depth of thread h and corresponding change (h_{nom}=0.812 mm)

No.	Depth of thread h, mm	$\Delta h = h_{nom} - h$, mm	Change, %
1	0.802	0.01	1.23
2	0.804	0.008	0.99
3	0.806	0.006	0.74
4	0.8	0.012	1.48
5	0.808	0.004	0.49
6	0.818	−0.006	−0.74
7	0.806	0.006	0.74
8	0.798	0.014	1.72
9	0.808	0.004	0.49
10	0.806	0.006	0.74
Average	0.8056	0.006	0.788
Standard deviation	0.0055	0.0055	0.675

−4.296 and 0.788% respectively. It is interesting that the shrinkage for thread pitch is a negative value, meaning that the thread pitch increases. This is because water expands along the axial direction of the bolt during freezing, while silicon rubber is soft and cannot exert a constraint on this expansion. These errors can be reduced by modifying pattern dimensions, i.e. incorporating a 'shrinkage factor' to improve the dimensional accuracy.

Conclusions

The present paper describes the experimental results of the fracture toughness of mould material generated for investment casting with ice patterns in a low temperature environment. The effects of various parameters on the fracture toughness have been investigated. The parameters considered include the ratio of fused silica *v.* aluminosilicate, the volume of binder and the volume of catalyst. The Taguchi method was used to reduce the number of trial runs required for four point bend analysis of bars made with variations of these materials. The analysis of variance shows that the fracture toughness of the ceramic increases with an increase in the amount of fibre containing fused silica when the added fused silica is larger than a critical value. The toughness also increases with a decrease in the amount of binder. The SEM analysis demonstrates that the addition of fused silica with fibres can strengthen the mould material and consequently, make crack free moulds. Based on the above analysis, sound moulds have been made for the investment casting process with ice patterns. An M8 bolt is used as an example to demonstrate that investment casting with ice patterns can be used to fabricate parts with complex geometry and achieve good dimensional accuracy.

Acknowledgement

The authors gratefully acknowledge the financial support from the National Science Foundation grants DMI-0128313, DMI-0140625 and DMI-0321712.

References

1. P. R. Beeley and R. F. Smart: 'Investment casting', 1st edn; 1995, Cambridge, The University Press.
2. V. L. Richards and B. V. Sunderland: Proc. 49th Annual Technical Meeting, Orlando, FL, USA, October 2001, Investment Casting Institute, 2:1–12.
3. A. Yodice: US patent 5,072,770, 1991.
4. A. Yodice: *INCAST: Int. Mag. Invest. Cast. Inst.*, 1998, **11**, 19–21.
5. D. M. Peters: *Foundry Manage. Technol.*, 1995, **123**, (90–91), 96.
6. X. Wu: 'Study on ceramic mold investment casting based on ice patterns made by rapid prototyping method', Bachelor's dissertation, Tsinghua University, Beijing, China, 1997.
7. M. C. Leu, Q. Liu and F. D. Bryant: *Ann. CIRP*, 2003, **52**, 185–188.
8. Q. Liu, G. Sui and M. C. Leu: *J. Comput. Ind.*, 2002, **48**, 181–197.
9. Q. Liu and M. C. Leu: Proc. International Mechanical Engineers Congress and Exposition, Anaheim, CA, USA, November 2004, American Society of Mechanical Engineering, Paper IMECE2004-59580.
10. W. Zhang, M. C. Leu, Z. Ji and Y. Yan: US patent 6,253,116, 2001.
11. Q. Liu, M. C. Leu, V. L. Richards and S. M. Schmitt: *Int. J. Adv. Manuf. Technol.*, 2004, **24**, 485–495.
12. Q. Liu and M. C. Leu: Proc. Conf. on 'Materials and process for medical devices', Anaheim, CA, USA, September 2003, ASM International, 438–443.
13. M. C. Leu and Q. Liu: Proc. NSF Design, Service and Manufacturing Grantees and Research Conference, Birmingham, AL, USA, January 2003, The University of Alabama.
14. Q. Liu and M. C. Leu: Proc. Symp. on 'Solid freeform fabrication', Austin, TX, USA, August 2002, University of Texas at Austin, 563–574.
15. Q. Liu, M. C. Leu, V. Richards and H. Jose: Proc. 15th Symp. on 'Solid freeform fabrication', Austin, TX, USA, August 2004, University of Texas at Austin, 602–611.
16. 'Standard test method for flexural strength of advanced ceramics at ambient temperature', C 1161-02c, ASTM, Philadelphia, PA, USA, 2002.
17. F. I. Baratta: 'Requirements for flexure testing of brittle materials', AMMRC TR 82-20, Army Materials and Mechanics Research Center, Watertown, MA, USA, 1982.
18. V. L. Richards and G. Connin: Proc. 49th Annual Technical Meeting, Orlando, FL, USA, October 2001, Investment Casting Institute, Paper 13.
19. D. R. Askeland: 'The science and engineering of materials', 3rd edn; 1989, Boston, MA, PWS Publishing Company.
20. K. Kendall, N. McN Alford, S. R. Tan and J. D. Birchall: *J. Mater. Res.*, 1986, **1**, 120–123.
21. V. L. Richards and S. Mascreen: Proc. 50th Technical Conference and Expo, Chicago, IL, USA, September–October 2002, Investment Casting Institute.
22. G. E. Dieter: 'Mechanical metallurgy', 3rd edn; 1986, New York, McGraw-Hill Book Company.
23. M. L. Williams: *J. Appl. Mech.*, 1957, **24**, 109–114.
24. G. R. Irwin: *J. Appl. Mech.*, 1957, **24**, 361–364.
25. W. Y. Fowlkes and C. M. Creveling: 'Engineering methods for robust product design', 1995; Boston, MA, Addison-Wesley Publishing Company.
26. J. B. Wachtman: 'Mechanical properties of ceramics'; 1996, New York, Wiley-Interscience Publications.
27. Investment Casting Institute: 'Investment casting handbook'; 1980, Chicago, IL, Investment Casting Institute.